JPET Fast Forward. Published on February 8, 2006 as DOI: 10.1124/jpet.105.098210

Expression profiles of high voltage-activated calcium channels in sympathetic and parasympathetic pelvic ganglion neurons innervating the urogenital system

Yu-Jin Won, Kum Whang, In Deok Kong, Kyu-Sang Park,

Joong-Woo Lee, and Seong-Woo Jeong

Departments of Physiology (*Y.-J.W, I.D.K, K.-S.P, J.-W.L., S.-W.J.*) and Neurosurgery (*K.W.*), Institute of Basic Medical Science, Yonsei University Wonju College of Medicine, Wonju, Kangwon-Do 220-701, Republic of Korea

Identification of calcium channel isoforms in MPG neurons

Corresponding Author:
Seong-Woo Joeng, Ph.D.
Department of Physiology
Yonsei University Wonju College of Medicine,
Wonju, Kangwon-Do 220-701
Republic of Korea
Tel) +82-33-741-0293
Fax) +82-33-745-6461
e-mail) swjeong@wonju.yonsei.ac.kr

No. of text pages: 37
No. of tables: 1
No. of figures: 5
No. of references: 40
No. of words in the Abstract: 248
No. of words in the Introduction: 495
No. of words in the Discussion: 1281

Abbreviation:
AHP, afterhyperpolarization; EBSS, Earle's balanced salt solution; HEK, human embryonic kidney; HVA, high voltage-activated; MEM, minimal essential medium; LVA, low voltage-activated; RT-PCR, reverse transcription-polymerase chain reaction; VACCs, voltage-activated Ca^{2+} channels.

Recommended section: Cellular and Molecular

JPET Fast Forward. Published on February 8, 2006 as DOI: 10.1124/jpet.105.098210
This article has not been copyedited and formatted. The final version may differ from this version.

ABSTRACT

Among the autonomic ganglia, major pelvic ganglia (MPG) innervating the urogenital system are unique since both sympathetic and parasympathetic neurons are co-localized within one ganglion capsule. Sympathetic MPG neurons are discriminated from parasympathetic ones by expression of low voltage-activated Ca^{2+} channels that primarily arise from T-type α_{1H} isoform and contribute to generation of low-threshold spikes. Until now, however, expression profiles of high voltage-activated (HVA) Ca^{2+} channels in these two populations of MPG neurons remain unknown. In the present study, thus, we dissected HVA Ca^{2+} channels out using pharmacological and molecular biological tools. RT-PCR analysis showed that MPG neurons contained transcripts encoding all known HVA Ca^{2+} channel isoforms (α_{1B}, α_{1C}, α_{1D} and α_{1E}) except α_{1A}. Western blot analysis and pharmacology with ω-agatoxin IVA (1 μM) confirmed that MPG neurons lack the α_{1A} Ca^{2+} channels. Unexpectedly, the expression profile of HVA Ca^{2+} channel isoforms was identical in the sympathetic and parasympathetic neurons of the MPG.. Of the total Ca^{2+} currents, ω-conotoxin GVIA-sensitive N-type (α_{1B}) currents constituted 57±5% (n=9) and 60±3% (n=6), respectively; nimodipine-sensitive L-type (α_{1C} and α_{1D}) currents made up 17±4% and 14±2%, respectively; and nimodipine- and ω-conotoxin GVIA-resistant R-type currents were 25±3% and 22±2%, respectively. The

JPET Fast Forward. Published on February 8, 2006 as DOI: 10.1124/jpet.105.098210
This article has not been copyedited and formatted. The final version may differ from this version.

R-type Ca^{2+} currents were sensitive to $NiCl_2$ (IC_{50}=22±0.1 μM), but not to SNX-482 which was able to potently (IC_{50}=76±0.4 nM) block the recombinant $\alpha_{1E}/\beta_{2a}/\alpha_2\delta$ Ca^{2+} currents expressed in HEK 293 cells. Taken together, our data suggest that sympathetic and parasympathetic MPG neurons share a similar but unique profile of HVA Ca^{2+} channel isoforms.

JPET Fast Forward. Published on February 8, 2006 as DOI: 10.1124/jpet.105.098210
This article has not been copyedited and formatted. The final version may differ from this version.

Introduction

Voltage-activated Ca^{2+} channels (VACCs) allow Ca^{2+} influx in response to membrane depolarization and mediate diverse neural functions including transmitter release and excitability. In general, VACCS are composed of α1 subunit and differential auxiliary subunits, β, $\alpha_2\delta$, and γ. Until now, molecular cloning studies have revealed ten distinct genes encoding different α_1 subunits which are now classified into three subfamilies: $Ca_v1(\alpha_{1C}, \alpha_{1D}, \alpha_{1F}, \alpha_{1S})$, $Ca_v2(\alpha_{1A}, \alpha_{1B}, \alpha_{1E})$, and $Ca_v3(\alpha_{1G}, \alpha_{1H}, \alpha_{1I})$ (Catterall et al. 2003). The Ca_v1 subfamily encodes high voltage-activated (HVA) L-type channels. Of the Ca_v2 subfamily, α_{1A}, α_{1B}, and α_{1E} genes correspond to HVA P/Q-, N-, and R-type channels, respectively. The members of the Ca_v3 subfamily correspond to low voltage-activated (LVA) T-type Ca^{2+} channels. Generally, each neural tissue displays its own expression profile of VACCs. Since HVA Ca^{2+} channels, i.e. L-, N-, P-, Q-, and R-types, show overlapping biophysical properties, use of specific pharmacological tools is crucial in probing each type of HVA Ca^{2+} channel. Briefly, L-type Ca^{2+} channels can be identified by use of dihydropyridines such as nifedipine (Bean 1984). N-type channels are highly sensitive to ω-conotoxin GVIA isolated from the fish-hunting sea snail (Olivera et al. 1994). P- and Q-type channels are identified by application of a spider toxin, ω-agatoxin IVA at low and high concentrations,

respectively (Bourinet et al. 1999). R-type channels are originally defined as residual Ca^{2+} channels resistant to the combined application of the organic and peptide channel blockers (Zhang et al., 1993), and are found to be relatively more sensitive to nickel than other HVA Ca^{2+} channels. Recently, another spider toxin called SNX-482 is available for selectively blocking R-type calcium channels (Newcomb et al., 1998). However, splicing variants of R-type Ca^{2+} channels resistant to SNX-482 have been also described in some central nervous system neurons such as retinal ganglion neurons, hippocampal CA1 neurons, and cerebellar granule neurons (Newcomb et al. 1998; Tottene et al. 2000; Sochivko et al. 2002).

The pelvic ganglia provide autonomic innervation to the urogenital system including the descending colon, the urinary bladder, and the external genitalia and mediate visceral reflexes such as micturition and penile erection (Dail et al., 1983). The most prominent feature of the pelvic ganglia is that both sympathetic and parasympathetic neurons reside in the same ganglion capsule (Keast, 1995)(Keast, 1995). Interestingly, low voltage-activated (LVA) T-type Ca^{2+} channels are exclusively expressed in sympathetic major pelvic ganglia (MPG) neurons of rat (Zhu et al. 1995), which has never been reported for other autonomic ganglion neurons. Recently, we have shown that T-type Ca^{2+} channels mainly arise from the Ni^{2+} and Zn^{2+}-sensitive α_{1H} isoform,

and contribute to generation of low-threshold spikes in sympathetic MPG neurons (Lee et al., 2002; Jeong et al. 2003). To date, however, it still remains unknown which isoforms of HVA Ca^{2+} channels are functionally expressed in MPG neurons and, more importantly, whether the expression profile of HVA Ca^{2+} channels is cell-specific. In present study, thus, we dissected HVA Ca^{2+} channels out in MPG neurons using pharmacological and molecular biological tools.

Materials and Methods

Isolation of MPG neurons. All the animal studies were conducted according to the National Institutes of Health's *Guidelines* for Care and Use of Experimental Animals. Single neurons of the MPG were enzymatically dissociated as described previously (Lee et al. 2002). Briefly, male Sprague-Dawley rats (150-200g) were anesthetized with pentobarbital sodium (50 mg/kg i.p.). The MPG were dissected out from the lateral surface of the prostate gland and placed in cold Hank's balanced salt solution. The ganglia were then desheathed, cut into small pieces, and incubated in the modified Earle's balanced salt solution (EBSS, pH 7.4) containing 0.7 mg/ml collagenase type D, 0.1 mg/ml trypsin (all from Boehringer Mannheim Biochemicals, Indianapolis, IN), and 0.1 mg/ml DNase Type I (Sigma Chemical Co., St Louis, MO) at 35 °C for 55 min. The

EBSS was modified by adding 3.6 gm/L glucose, and 10 mM HEPES. After incubation, neurons were dissociated by vigorous shaking of the flask. After centrifugation at 50 × g for 5 min, the dissociated neurons were resuspended in minimum essential medium (MEM) containing 10% fetal bovine serum (FBS) and 1% penicillin-streptomycin (all from Cambrex Bio Science, Inc, Walkersville, MD). These same procedures for cell preparation were used in all experiments including RT-PCR, Western blot, and electrophysiology as shown before (Lee et al. 2002). For electrophysiological measurements of currents, neurons were then plated onto culture dishes (35mm) coated with poly-D-lysine and maintained in a humidified 95% air-5% CO_2 incubator at 37 °C. Current recordings were made within 6 hr after dissociation.

Transient expression of Ca^{2+} channels in HEK 293 cells. The plasmid cDNAs **e**ncoding rat α_{1E} (rbEII, accession number L15453) were in pMT2 (Genetics Institute, Cambridge, MA), rat β_{2a} (M80545) (Perez-Reyes et al., 1992) and rat $\alpha_2\delta$ (M86621) (Kim et al. 1992) were in pCDNA3 (Invitrogen, Carlsbad, CA), and green fluorescence protein (GFP) were in pEGFP-N1 (Clontech, Cambridge, UK). The human embryonic kidney (HEK) 293 cells were grown in standard Dulbecco's modified Eagle's medium (Invitrogen,) supplemented with 10% FBS (Cambrex), 100 μg/mL streptomycin, and 100 units/mL penicillin (Cambrex). HEK 293 cells which had 90% confluency, were

dissociated with trypsin-EDTA and replated on 35 mm dishes (Corning) with a density of 2×10^5 cells/dish. One day after plating, these cells were transfected with 1, 0.5, 1, and 0.7 μg of α_{1E}, β_{2a}, $\alpha_2\delta$, and GFP cDNAs, respectively, using a calcium phosphate transfection kit (Invitrogen). These cells were then incubated for at least 24 hr in CO_2 incubator at 37 °C. Successfully transfected cells were identified by green fluorescence, and electrophysiological recordings were made between 2 and 4 days after transfection.

RT-PCR analysis. Total RNA of the dissociated MPG neurons was extracted using Trizol reagent (Invitrogen, Carlsbad, CA, USA). The first strand cDNA was synthesized from 1 μg of total RNA using 50 U M-MLV reverse transcriptase (PerkinElmer Life Sciences, Shelton, CT, USA) by 1 hr incubating at 42°C. The PCR reaction was initiated by the initial denaturation at 95°C for 15 min, followed by 35 cycles consisting of 94°C for 60 s, 55°C for 45 s, and 72°C for 60 s. The PCR reaction was completed by maintaining temperatures at 72°C for 10 min. As an internal reference, GapDH gene was amplified. The resultant PCR products were separated on a 1.5% agarose gel and visualized by ethidium bromide staining. Specific primer pairs are listed in Table 1.

Western blotting. The dissociated MPG neurons, and rat whole brain and cerebellar tissues (used for positive controls) were homogenized in ice-cold hypotonic buffer (10 mM Tris, pH 7.4) containing protease inhibitor cocktail (Sigma), and then were

centrifuged at 13,000 rpm for 10 min. The cocktail solution contained (in mM) 104 4-(2-aminoethyl) benzenesulfonyl fluoride (AEBSF), 0.08 aprotinin, 2 leupeptin, 4 bestatin, 1.5 pepstatin A, and 1.4 E-64. The precipitated samples were resolved in a lysis buffer (50 mM Tris-HCl, 150mM NaCl, 1% NP40, and protease inhibitor, pH 8.0), incubated for 40 min on ice, and then centrifuged at 13000 rpm for 15 min to remove any insoluble material. Aliquots were taken to quantify total lysate protein using the Bradford method. After boiling in SDS buffer for 5 min, samples (40 μg protein/lane) were separated by SDS-PAGE using 8% acrylamide gel and then transferred (150 V for 1hr) to polyvinylidene difluoride membrane (BioTrace^{TM} PVDF, PALL Corporation, USA). The membrane was blocked with TTBS (Tween-Tris-buffered saline) containing 2% BSA for 30 min, incubated overnight at 4°C with rabbit polyclonal antibodies directed against the II-III linkers of Ca^{2+} channel α_{1A}, α_{1B}, α_{1C}, α_{1D}, and α_{1E} subunits (all from Alomone labs, Jerusalem, Israel) at working dilution of 1:200, and washed several times with TTBS containing 1% Tween 20. Horseradish-peroxidase conjugated secondary antibody was added and then membranes were incubated for 1 hr at room temperature. After extensive washing, bound antibodies were detected by ECL western blotting detection reagents (Amersham Biosciences, Little Chalfont, UK) on X-ray film.

Electrophysiological recordings. From the acutely dissociated MPG neurons, Ca^{2+}

currents were recorded using the whole cell-ruptured configuration of the patch clamp technique (Hamill et al. 1981) as described previously (Jeong and Ikeda, 1998). The sympathetic and parasympathetic MPG neurons were identified by the presence or absence of both T-type Ca^{2+} and GABA currents, respectively (see more details in Results). Patch electrodes were fabricated from a borosilicate glass capillary (Corning 7052, Garner Glass Co. Claremont, CA, USA). The electrodes were coated with Sylgard 184 (Dow corning, Midland, MI, USA), and fire polished on microforge. The electrodes had resistances of 1.5-2.5 MΩ after filling with the internal solution described below. An Ag/AgCl pellet connected via a 0.15 M NaCl/agar bridge was used to ground the bath. The cell membrane capacitance and series resistance were compensated (>80%) electronically using an Axopatch-1D amplifier (Axon Instruments, Foster City, CA, USA). Voltage protocol generation and data acquisition were performed using S5 data acquisition software (written by Dr. Stephen R. Ikeda) on a Macintosh G4 computer equipped with an ITC18 data acquisition board (Instrutech, Port Washington, NY, USA). Current traces were generally low-pass filtered at 5 KHz using the 4-pole Bessel filter in the clamp amplifier, digitized at 2 KHz, and stored on the computer hard drive for later analysis. All experiments were performed at room temperature (20~24 °C).

Solutions and drugs. To isolate Ca^{2+} currents, patch pipettes were filled with an

JPET Fast Forward. Published on February 8, 2006 as DOI: 10.1124/jpet.105.098210
This article has not been copyedited and formatted. The final version may differ from this version.

internal solution containing (in mM): 120 N-methyl-D-glucamine (NMG)-methanesulfonate (MS), 20 tetraethylammonium (TEA)-MS, 20 HCl, 11 EGTA, 1 $CaCl_2$, 10 HEPES, 4 Mg-ATP, 0.3 Na_2-GTP, and 14 creatine phosphate (pH 7.2). External recording solution contained (in mM): 145 TEA-MS, 10 HEPES, 10 $CaCl_2$, 15 glucose, and 0.0003 tetrodotoxin (TTX) (pH 7.4). Drugs were applied to single neurons via a gravity-fed fused silica capillary tube connected to an array of seven polyethylene tubes. Stock solutions (0.1-10 mM) were made for the following drugs: nimodipine (Sigma), ω-agatoxin IVA, ω-conotoxin GVIA, SNX-482 (all from Alomone Labs, Jerusalem, Israel), $CdCl_2$, and $NiCl_2$. All peptides were stored at -20 ℃ or -80 ℃. These drugs were dissolved in distilled water, except for nimodipine which was dissolved in DMSO. For experiments with toxins, the external solution was supplemented with cytochrome C (0.1 mg/ml) to minimize nonspecific peptide binding. Cytochrome C itself had no effect on Ca^{2+} currents.

Data analysis. Current traces were corrected for linear leakage current as determined by hyperpolarizing pulses. The membrane capacitance was measured by application of a 10-mV hyperpolarizing pulse from a holding potential of -80 mV and calculated in according to the following equation: $C_m = \tau_c I_o/\triangle V_m (1-I_\infty/I_o)$, where C_m is the membrane capacitance, τ_c is the time constant of membrane capacitance, I_o is the

JPET Fast Forward. Published on February 8, 2006 as DOI: 10.1124/jpet.105.098210
This article has not been copyedited and formatted. The final version may differ from this version.

maximum capacitive current value, $\triangle V_m$ is the amplitude of test pulse, and I_∞ is the amplitude of steady-state current (see Jeong and Wurster, 1997). Concentration-response curves were constructed by fitting experimental data to the Hill equation: $B=B_{max}/(1+(IC_{50}/[drug]/)^n)$ where B is the fraction blocked, B_{max} is the maximal block, IC_{50} is the half-maximal inhibitory concentration of the drug applied, and n is the Hill slope. Data analysis and curve fitting were performed with the IGOR data analysis package (Wave-Metrics, Lake Oswego, OR). Data were presented as means±SEM.

Results

Molecular identification of HVA Ca^{2+} channel isoforms expressed in MPG neurons.

To determine the expression profile of transcripts encoding HVA Ca^{2+} channel α_1 subunits, RT-PCR analysis was performed on mRNAs isolated from the dissociated MPG neurons. As a positive control, mRNAs from whole rat brain tissues were RT-PCR amplified. As illustrated in Fig.1, MPG neurons expressed transcripts for all HVA Ca^{2+} channel α_1 subunits (i.e., α_{1B}, α_{1C}, α_{1D} and α_{1E}) except α_{1A}. As previously reported (Lee et al. 2002), MPG neurons also contained transcripts for the T-type Ca^{2+} channel α1H. When the RT-PCR process was run without reverse transcriptase (RT-), no PCR products were observed indicating no contamination of genomic DNAs (Fig.1). The

JPET Fast Forward. Published on February 8, 2006 as DOI: 10.1124/jpet.105.098210
This article has not been copyedited and formatted. The final version may differ from this version.

mRNA transcript for α_{1A} was clearly detected in RT-PCR products of the positive control as a band of the expected size (lane1, 332 bp). We next carried out Western blotting to examine whether all detected mRNA transcripts were translated into the corresponding Ca^{2+} channel α_1 subunits in the exactly same preparation of MPG neurons as used for RT-PCR and electrophysiology. All primary antibodies applied in these experiments have been proven to be highly specific (Saegusa et al. 2000; Latour et al. 2003). As positive controls, proteins extracted from whole brain (for α_{1A}, α_{1B}, α_{1C} and α_{1D}) and cerebellar tissues (for α_{1E}) were employed. Consistent with the RT-PCR results, MPG neurons expressed α_{1B}, α_{1C}, α_{1D}, and α_{1E}, but not α_{1A} proteins (Fig.2). In the present study, contamination of non-neuronal cells, if any, could not be completely prevented in the MPG preparation. However, the results acquired from the RT-PCR and Western blotting analyses were consistent with the electrophysiological data acquired in single MPG neurons as described below.

Pharmacological identification of HVA Ca^{2+} channel isoforms expressed in sympathetic and parasympathetic MPG neurons. Cell types of the MPG neurons could be easily recognized according to the previously established criteria: cell size as assessed by electrical capacitance measurements and expression of T-type Ca^{2+} channels (Zhu and Yakel 1997, Zhu et al. 1995, Lee et al. 2002). As illustrated in Figure 3A, we

JPET Fast Forward. Published on February 8, 2006 as DOI: 10.1124/jpet.105.098210
This article has not been copyedited and formatted. The final version may differ from this version.

could identify the sympathetic MPG neurons by the presence of T-type Ca^{2+} currents detected as a prominent hump at low-voltage range (-50 to -20 mV) or fast-inactivating peak currents evoked by test pulses to -30 mV. Conversely, the parasympathetic MPG neurons lack the hump and transient T-type Ca^{2+} currents. To make sure of the identified cell type, we further tested the presence or absence of responses to γ-amino butyric acid (GABA) in the same cell in which Ca^{2+} currents were recorded. Application of 0.1 mM GABA evoked a large inward Cl^- current in sympathetic MPG neurons expressing T-type Ca^{2+} currents. The inward GABA currents were reversed around 0 mV since concentrations of Cl^- ions (20 mM) were same in the external and internal solutions for Ca^{2+} current recording (data not shown). Conversely, the GABA currents were negligible in parasympathetic MPG neurons lacking in T-type Ca^{2+} currents (Fig. 3B). The average capacitances of the sympathetic and parasympathetic MPG neurons tested were 61±11 pF (n=44) and 29±12 pF (n=21), respectively. Thus, in the following experiments, we identified MPG neurons as sympathetic if they showed both T-type Ca^{2+} currents and the GABA response, and as parasympathetic if they did not.

Next, we addressed the following two questions: what subtypes of HVA Ca^{2+} channels were functionally expressed and whether the expression is cell type-specific as determined by the presence of T-type Ca^{2+} channel current (Lee et al. 2002). In this

regard, HVA Ca^{2+} currents were pharmacologically dissected out in sympathetic and parasympathetic MPG neurons by sequential application of different toxins and drugs (Adams et al. 1993; Randall and Tsien, 1995). To evoke the peak Ca^{2+} currents, test pulses to +10 mV were applied from a holding potential of -80 mV at 0.1 Hz. During current measurements for 10 min, no significant run down in the peak Ca^{2+} current was detected (data not shown). Figure 4A represents time-dependent reductions in Ca^{2+} currents by different subtype-specific antagonists in a sympathetic MPG neuron. Application of nimodipine (10 μM), a DHP L-type antagonist, blocked 21% of total Ca^{2+} currents. The N-type current was identified with the use of ω-conotoxin GVIA isolated from the venom of the fish-hunting snail, *Conus geographus* (Olivera et al. 1984). In the presence of ω-conotoxin GVIA at a saturating concentration (2 μM), 54% of total Ca^{2+} currents was slowly blocked. After successively blocking L- and N-type Ca^{2+} currents, we tested with a high concentration of ω-agatoxin IVA (1 μM), which was large enough to block both P- and Q-types of currents (Randall and Tsien, 1995; Jeong and Wurster, 1997). However, no currents were affected by ω-agatoxin IVA in the sympathetic neuron. In addition, application of ω-conotoxin MVIIC (1 μM), a N- and P/Q-type antagonist, failed to block the Ca^{2+} currents further in presence of nimodipine and ω-conotoxin GVIA (data not shown). These results were consistent with absence of

JPET Fast Forward. Published on February 8, 2006 as DOI: 10.1124/jpet.105.098210
This article has not been copyedited and formatted. The final version may differ from this version.

the α1A transcript and protein as revealed by RT-PCR and western blotting analyses. There remained significant residual currents resistant to the combined application of the organic antagonists. These residual currents were fully blocked by $CdCl_2$ (0.1 mM), a non-selective Ca^{2+} channel antagonist, indicating presence of R-type Ca^{2+} currents (Fig. 4A). Taken together, the sympathetic MPG neuron was found to functionally express three types (L-, N-, and R-type) of HVA Ca^{2+} channels but not the P/Q-types.

We also examined inhibitory effects of nimodipine (10 μM), ω-conotoxin GVIA (2 μM), agatoxin IVA (1 μM), and $CdCl_2$ (0.1 mM) on HVA Ca^{2+} currents in the parasympathetic neurons showing no T-type Ca^{2+} and GABA currents (Fig. 4B). Like the sympathetic MPG neurons, the parasympathetic MPG neurons functionally expressed L-, N-, and R- except P/Q-type Ca^{2+} currents. As summarized in Fig. 4C, there was no cell-specific difference in the relative contribution of the Ca^{2+} channel isoforms to total Ca^{2+} currents. On average, L-type Ca^{2+} channels contribute to 17±4% and 14±2%, N-type to 57±5% and 60±3%, and R-type to 25±3% and 22±2% of the total currents, respectively, in sympathetic (n=16) and parasympathetic (n=13) MPG neurons. It should be mentioned that the current kinetics were not further analyzed to characterize the pharmacologically identified Ca^{2+} channel subtypes because the kinetics appeared to be variable from one cell to the next.

JPET Fast Forward. Published on February 8, 2006 as DOI: 10.1124/jpet.105.098210
This article has not been copyedited and formatted. The final version may differ from this version.

Pharmacological characteristics of R-type Ca^{2+} currents in MPG neurons. A previous study has shown that native R-type Ca^{2+} currents could be potently blocked by nickel (Tottene et al, 1996). Accordingly, we tested effects of nickel on R-type Ca^{2+} currents. When nickel (0.3 mM) was applied after blocking L- and N-types with nimodipine (10 μM) and ω-conotoxin GVIA (2 μM), the R-type Ca^{2+} currents were significantly blocked in a sympathetic MPG neuron (Fig. 5A). On average, nickel at 0.3 mM blocked 72±4% (n=3) of the MPG R-type Ca^{2+} currents. Interestingly, SNX-482 (500 nM), a selective antagonist of recombinant α1E channels, failed to produce effective block of the native R-type currents (n=16). Likewise, in parasympathetic MPG neurons, R-type currents were sensitive to nickel but not SNX-482 (data not shown). Next, we compared the pharmacological properties of the MPG R-type Ca^{2+} currents with that of the prototype α1E (rbEII) heterologously expressed in HEK 293 cells (Fig. 5B). No endogenous Ca^{2+} currents were detected in control cells expressing only GFP, while large peak Ca^{2+} currents were developed in cells co-expressing rat α1E, β_{2a}, and $\alpha_2\delta$ subunits. The peak Ca^{2+} currents of the recombinant α1E were very sensitive to both nickel and SNX-482, which is consistent with the previous findings (Soong et al. 1993; Zamponi et al. 1996; Newcomb et al. 1998). On average, nickel at 0.3 mM and SNX-482 at 300 nM blocked 70±5% (n=3) and 94±3% (n=3) of the recombinant α1E

Ca^{2+} currents, respectively. As defined from concentration-response curves (Fig. 5C), the potency (IC_{50}) of Ni^{2+} block was similar for the MPG R-type (22±1.1 μM; slope factor, 0.81±0.11) and the recombinant α1E (21±0.2 μM; slope factor, 0.75±0.13) Ca^{2+} currents. More importantly, unlike the MPG R-type, the recombinant α1E Ca^{2+} currents expressed in HEK 293 cells were highly sensitive to SNX-482 (IC_{50}=76±0.4 nM; slope factor, 1.71±0.25) (Fig. 5D). The Hill slope factor suggests that the recombinant α1E may have more than SNX-482 site, as previously reported (Tottene et al. 2000). Taken together, our data suggest that MPG neurons express Ni^{2+}-sensitive and SNX 482-resistant R-type Ca^{2+} currents.

Discussion

In the present study, we have three major findings that (1) MPG neurons express L-, N-, R-type, but not P/Q-type Ca^{2+} channels, (2) unlike that of LVA T-type Ca^{2+} channels, expression profile of HVA Ca^{2+} channels was identical in both sympathetic and parasympathetic MPG neurons, and (3) the native R-type Ca^{2+} channels were resistant to SNX-482 which is capable of potently blocking the recombinant α1E channels.

Cell type-independent expression of HVA Ca^{2+} channel subtypes. MPG provides a good model system for studying cell-specific gene expression and functions (e.g.,

JPET Fast Forward. Published on February 8, 2006 as DOI: 10.1124/jpet.105.098210
This article has not been copyedited and formatted. The final version may differ from this version.

tonic vs. phasic firing patterns) in the autonomic nervous system because one ganglion capsule possesses both sympathetic and parasympathetic neurons (Dail 1992). The impetus for the present study arose from previous findings that LVA T-type Ca^{2+} channels encoded by the α1H are exclusively expressed in sympathetic MPG neurons (Zhu et al. 1995, Lee et al. 2002). Accordingly, we speculated that expression profile of HVA Ca^{2+} channel subtypes could be different between sympathetic and parasympathetic MPG neurons, which may affect neuronal functions. In conjunction with Western blotting analysis, however, pharmacological studies with nimodipine, ω-conotoxin GVIA, and ω-agatoxin IVA indicate that the expression profile of HVA Ca^{2+} channels is identical for two populations of MPG neurons, although functional roles of certain subtypes appear to be cell-specific (see below).

Characteristics of HVA Ca^{2+} channel expression. The total Ca^{2+} channel currents are commonly comprised of L-, N-, and R-type currents. In MPG neurons, N-type Ca^{2+} channel is the dominant subtype responsible for 60% of the total currents, which is comparable with other mammalian autonomic neurons including sympathetic superior cervical (Boland et al. 1994; Zhu et al. 1995), coeliac-superior mesenteric (Carrier and Ikeda, 1992), parasympathetic intracardiac (Xu and Adams, 1992; Jeong and Wurster, 1997), and paratrachial (Aibara et al. 1992) neurons. L-type Ca^{2+} currents mediate about

JPET Fast Forward. Published on February 8, 2006 as DOI: 10.1124/jpet.105.098210
This article has not been copyedited and formatted. The final version may differ from this version.

15 % of total Ca^{2+} currents and appear to arise from both α1C and α1D isoforms. In MPG neurons substantial currents (25% of total currents) were resistant to application of nimodipine and ω-conotoxin GVIA. Most autonomic neurons are known to display the non-L and non-N-type currents (Adams and Harper 1995). However, so far, the nature of these currents has been poorly defined (but see Jeong and Wurster, 1997), but they are expected to consist of P-, Q-, and R-type Ca^{2+} currents. Although both P- and Q-type Ca^{2+} channels are the α_{1A} gene products, biophysical and pharmacological phenotypes are quite different. This may be due to the differential splicing of the α1A subunit (Bourinet et al. 1999) and/or its association with different β subunits (Moreno et al. 1997; Mermelstein et al. 1999). Noninactivating P-type Ca^{2+} channels are potently blocked by ω-agatoxin IVA (IC_{50} = ~1 nM), while Q-type Ca^{2+} channels with fast kinetics are less sensitive to the toxin (IC_{50} = ~100 nM) (Randall and Tsien, 1995). In our experiments RT-PCR and Western blotting analyses failed to detect the α_{1A} transcript and protein. Consistent with these results, 1 μM ω-agatoxin IVA blocked none of the currents remaining in presence of nimodipine and ω-conotoxin GVIA. Taken together, we concluded that P/Q-type Ca^{2+} channels are absent in MPG neurons. Previous studies have shown that P/Q-type Ca^{2+} channels together with N-type channels mediate sympathetic and parasympathetic neurotransmission in rat vas deferens (Tran

and Boot, 1997; Wright and Angus, 1996) and bladder detrusor, respectively (Frew and Landy, 1995) (For review, see also Watermen 2000). Accordingly, it is likely that the P/Q-type Ca^{2+} channels are exclusively localized in synaptic terminals, but not in cell bodies of MPG neurons.

Pharmacological characteristics of R-type Ca^{2+} channels in MPG neurons. Overall, R-type Ca^{2+} currents appear to solely constitute the Cd^{2+}-sensitive non-L and non-N-type currents in MPG neurons. Western blotting analysis revealed expression of α1E proteins in MPG neurons. Similar to the recombinant α1E (rbEII) channels expressed in HEK 293 cells (Fig. 5; Zamponi et al. 1996) and Xenopus oocytes (Soong et al. 1993), R-type Ca^{2+} currents in MPG neurons were highly sensitive to Ni^{2+} block (IC_{50} = 22±0.1 μM). Accordingly, it is likely that the α1E underlies R-type Ca^{2+} currents in MPG neurons. The Ni^{2+} sensitivity of the R-type Ca^{2+} channels are similar to that of T-type Ca^{2+} channels previously reported (Lee et al, 2002; Jeong et al. 2003) and appear to be much higher than those of L- and N-type Ca^{2+} channels (Jeong et al. 2003). Interestingly, SNX-482, a selective antagonist of recombinant α1E channels, failed to block R-type Ca^{2+} currents in MPG neurons, which is also observed in several types of central neurons including rat cerebellar granule neurons (Newcomb et al. 1998). Recent studies using antisense or transgenic strategies have shown that the α1E gives rise to

both SNX-482-sensitive and SNX-482-resistant components (Piedras-Renteria and Tsien, 1998; Tottene et al. 2000; Sochivko et al.2002) whose relative contribution to R-type Ca^{2+} currents may vary from one cell to another cell. Like P/Q-type Ca^{2+} currents as explained above (Moreno et al. 1997; Bourinet et al. 1999), R-type Ca^{2+} currents showing different toxin sensitivity may also arise from alternative splicing and/or heterogeneity of Ca^{2+} channel auxiliary subunits. Indeed, some studies using RT-PCR analysis have revealed multiple splicing variants of the α1E gene in rat cerebellar granule neurons (Schramm et al. 1999) and human cerebellum (Pereverezev et al. 1998). On the other hand, it has been found that sensitivity of the recombinant α1E channel to SNX-482 is independent of Ca^{2+} channel β subunits (Bourinet et al. 2001) although effects of other auxiliary subunits, i.e., $\alpha_2\delta$ and γ subunits, remain unknown. In our preliminary experiment using RT-PCR analysis of mRNAs isolated from MPG neurons, we could detect a single splice variant containing a shorter II-III loop and longer N- and C-termini when compared with the cloned rat version (rbEII) (Won and Jeong, unpublished observation). This is reminiscent of rat cerebellar variants corresponding to SNX-482-resistant R-type Ca^{2+} currents (called “G3” or “Rc”) (Schramm et al. 1999). Taken together, at present, the most plausible explanation for resistance of R-type Ca^{2+} currents to SNX-482 in MPG neurons may employ alternative splicing of the prototype

α1E. However, one should note that the spliced loop and terminal regions can not interact with externally applied SNX-482. Recent study of Bourinet et al (2001) has suggested that candidate binding sites of SNX-482 may be the domain III and IV S3-S4 linker of the α1E subunit. Thus, it might be interesting to identify the splicing variant responsible for resistance to SNX-482 in MPG neurons.

Functional implications of HVA Ca^{2+} channels. Several studies have suggested that N- and P/Q-type, but not L-type Ca^{2+} channels mediate synaptic transmission between postganglionic neurons and effectors such as urinary detrusor and vas deferens (For review, see Waterman 2000). The roles of R-type Ca^{2+} channels in transmitter release are yet unclear. Previously, we have demonstrated that T-type Ca^{2+} channels are implicated in generation of low-threshold spikes in sympathetic MPG neurons (Lee et al. 2002). Likewise, the Ca^{2+} channel subtypes expressed in cell bodies of MPG neurons appear to contribute to spike adaptation in cell-specific ways. For example, L-type channel blocker, nimodipine greatly reduced the firing frequency through augmenting afterhyperpolarization (AHP) and I_{AHP} in the tonic sympathetic MPG neurons without affecting the phasic parasympathetic ones (Won and Jeong, unpublished observation). The functional roles of N- and R-type Ca^{2+} channels in regulation of excitability are now under investigation.

JPET Fast Forward. Published on February 8, 2006 as DOI: 10.1124/jpet.105.098210
This article has not been copyedited and formatted. The final version may differ from this version.

In summary, MPG neurons from adult rats express three distinct subtypes of HVA Ca^{2+} channels: L, N, and R types. The P/Q-type Ca^{2+} channels are not found in cell body although they are suggested to be localized in neuromuscular terminals (see above). The expression profile of HVA Ca^{2+} channels is identical in both sympathetic and parasympathetic neurons. The SNX-482-resistant R-type currents appear to result from alternative splicing of the α1E in MPG neurons.

References

Adams DJ and Harper AA (1995) Electrophysiological properties of autonomic ganglion neurons, in Autonomic Ganglia (McLachlan EM ed) pp153-212, Harwood, London.

Adams ME, Myers RA, Imperial JS and Olivera BM (1993) Toxityping rat brain calcium channels with omega-toxins from spider and cone snail venoms. *Biochemistry* **32**:12566-12570.

Aibara K, Ebihara S and Akaike N (1992) Voltage-dependent ionic currents in dissociated paratracheal ganglion cells of the rat. *J Physiol London* **457**:591-610.

Bean BP (1984) Nitrendipine block of cardiac calcium channels: high-affinity binding to the inactivated state. *Proc Natl Acad Sci U S A* **81**:6388-6392.

Boland LM, Morrill JA and Bean BP (1994) omega-Conotoxin block of N-type calcium channels in frog and rat sympathetic neurons. *J Neurosci* **14**:5011-5027.

Bourinet E, Soong TW, Sutton K, Slaymaker S, Mathews E, Monteil A, Zamponi GW, Nargeot J and Snutch TP (1999) Splicing of alpha 1A subunit gene generates phenotypic variants of P- and Q-type calcium channels. *Nat Neurosci* **2**:407-415.

Bourinet E, Stotz SC, Spaetgens RL, Dayanithi G, Lemos J, Nargeot J and Zamponi GW

(2001) Interaction of SNX482 with domains III and IV inhibits activation gating of alpha(1E) (Ca(V)2.3) calcium channels. *Biophys J* **81**:79-88.

Carrier GO and Ikeda SR (1992) TTX-sensitive Na^+ channels and Ca^{2+} channels of the L- and N-type underlie the inward current in acutely dispersed coeliac-mesenteric ganglia neurons of adult rats. *Pflügers Arch* **421**:7-16.

Catterall WA, Striessnig J, Snutch TP and Perez-Reyes E (2003) International Union of Pharmacology. XL. Compendium of voltage-gated ion channels: calcium channels. *Pharmacol Rev* **55**:579-581.

Frew R and Lundy PM (1995) A role for Q type Ca^{2+} channels in neurotransmission in the rat urinary bladder. *Br J Pharmacol* **116**:1595-1598.

Hamill OP, Marty A, Neher E, Sakmann B and Sigworth FJ (1981) Improved patch-clamp techniques for high-resolution current recording from cells and cell-free membrane patches. *Pflugers Arch* **391**:85-100.

Jeong SW and Ikeda SR (1998) G protein alpha subunit G alpha z couples neurotransmitter receptors to ion channels in sympathetic neurons. *Neuron* **21**:1201-1212.

Jeong SW, Park BG, Park JY, Lee JW and Lee JH (2003) Divalent metals differentially block cloned T-type calcium channels. *Neuroreport* **14**:1537-1540.

Jeong SW and Wurster RD (1997) Calcium channel currents in acutely dissociated intracardiac neurons from adult rats. *J Neurophysiol* **77**:1769-1778.

Keast JR (1995) Visualization and immunohistochemical characterization of sympathetic and parasympathetic neurons in the male rat major pelvic ganglion. *Neuroscience* **66**:655-662.

Kim HL, Kim H, Lee P, King RG and Chin H (1992) Rat brain expresses an alternatively spliced form of the dihydropyridine-sensitive L-type calcium channel alpha 2 subunit. *Proc Natl Acad Sci U S A* **89**:3251-3255.

Latour I, Hamid J, Beedle AM, Zamponi GW and Macvicar BA (2003) Expression of voltage-gated Ca^{2+} channel subtypes in cultured astrocytes. *Glia* **41**:347-353.

Lee JH, Kim EG, Park BG, Kim KH, Cha SK, Kong ID, Lee JW and Jeong SW (2002) Identification of T-type alpha1H Ca^{2+} channels ($Ca_v3.2$) in major pelvic ganglion neurons. *J Neurophysiol* **87**:2844-2850.

Mermelstein PG, Foehring RC, Tkatch T, Song WJ, Baranauskas G and Surmeier DJ (1999) Properties of Q-type calcium channels in neostriatal and cortical neurons are correlated with beta subunit expression. *J Neurosci* **19**:7268-7277.

Moreno H, Rudy B and Llinas R (1997) Beta subunits influence the biophysical and pharmacological differences between P- and Q-type calcium currents expressed in a

mammalian cell line. *Proc Natl Acad Sci U S A* **94**:14042-14047.

Newcomb R, Szoke B, Palma A, Wang G, Chen X, Hopkins W, Cong R, Miller J, Urge L, Tarczy-Hornoch K, Loo JA, Dooley DJ, Nadasdi L, Tsien RW, Lemos J and Miljanich G (1998) Selective peptide antagonist of the class E calcium channel from the venom of the tarantula Hysterocrates gigas. *Biochemistry* **37**:15353-15362.

Olivera BM, Miljanich GP, Ramachandran J and Adams ME (1994) Calcium channel diversity and neurotransmitter release: the omega-conotoxins and omega-agatoxins. *Annu Rev Biochem* **63**:823-867.

Pereverzev A, Klockner U, Henry M, Grabsch H, Vajna R, Olyschlager S, Viatchenko-Karpinski S, Schroder R, Hescheler J and Schneider T (1998) Structural diversity of the voltage-dependent Ca^{2+} channel alpha1E-subunit. *Eur J Neurosci* **10**:916-925.

Perez-Reyes E, Castellano A, Kim HS, Bertrand P, Baggstrom E, Lacerda AE, Wei XY and Birnbaumer L (1992) Cloning and expression of a cardiac/brain beta subunit of the L-type calcium channel. *J Biol Chem* **267**:1792-1797.

Piedras-Renteria ES and Tsien RW (1998) Antisense oligonucleotides against alpha1E reduce R-type calcium currents in cerebellar granule cells. *Proc Natl Acad Sci U S A* **95**:7760-7765.

Randall A and Tsien RW (1995) Pharmacological dissection of multiple types of Ca^{2+}

channel currents in rat cerebellar granule neurons. *J Neurosci* **15**:2995-3012.

Saegusa H, Kurihara T, Zong S, Minowa O, Kazuno A, Han W, Matsuda Y, Yamanaka H, Osanai M, Noda T and Tanabe T (2000) Altered pain responses in mice lacking alpha 1E subunit of the voltage-dependent Ca^{2+} channel. *Proc Natl Acad Sci U S A* **97**:6132-6137.

Schramm M, Vajna R, Pereverzev A, Tottene A, Klockner U, Pietrobon D, Hescheler J and Schneider T (1999) Isoforms of alpha1E voltage-gated calcium channels in rat cerebellar granule cells--detection of major calcium channel alpha1-transcripts by reverse transcription-polymerase chain reaction. *Neuroscience* **92**:565-575.

Sochivko D, Pereverzev A, Smyth N, Gissel C, Schneider T and Beck H (2002) The $Ca_V2.3$ Ca^{2+} channel subunit contributes to R-type Ca^{2+} currents in murine hippocampal and neocortical neurones. *J Physiol* **542**:699-710.

Soong TW, Stea A, Hodson CD, Dubel SJ, Vincent SR and Snutch TP (1993) Structure and functional expression of a member of the low voltage-activated calcium channel family. *Science* **260**:1133-1136.

Tottene A, Moretti A and Pietrobon D (1996) Functional diversity of P-type and R-type calcium channels in rat cerebellar neurons. *J Neurosci* **16**:6353-6363.

Tottene A, Volsen S and Pietrobon D (2000) Alpha(1E) subunits form the pore of three

cerebellar R-type calcium channels with different pharmacological and permeation properties. *J Neurosci* **20**:171-178.

Tran S and Boot JR (1997) Differential effects of voltage-dependent Ca^{2+} channels on low and high frequency mediated neurotransmission in guinea-pig ileum and rat vas deferens. *Eur J Pharmacol* **335**:31-36.

Waterman SA (2000) Voltage-gated calcium channels in autonomic neuroeffector transmission. *Prog Neurobiol* **60**:181-210.

Wright CE and Angus JA (1996) Effects of N-, P- and Q-type neuronal calcium channel antagonists on mammalian peripheral neurotransmission. *Br J Pharmacol* **119**:49-56.

Xu ZJ and Adams DJ (1992) Voltage-dependent sodium and calcium currents in cultured parasympathetic neurones from rat intracardiac ganglia. *J Physiol* **456**:425-441.

Zamponi GW, Bourinet E, and Snutch TP (1996) Nickel block of a family of neuronal calcium channels: subtype- and subunit-dependent action at multiple sites. *J Membrane Biol* **151**:77-90.

Zhang JF, Randall AD, Ellinor PT, Horne WA, Sather WA, Tanabe T, Schwarz TL and Tsien RW (1993) Distinctive pharmacology and kinetics of cloned neuronal Ca^{2+} channels and their possible counterparts in mammalian CNS neurons.

Neuropharmacology **32**:1075-1088.

Zhu Y and Yakel JL (1997) Modulation of Ca^{2+} currents by various G protein-coupled receptors in sympathetic neurons of male rat pelvic ganglia. *J Neurophysiol* **78**:780-789.

Zhu Y, Zboran EL and Ikeda SR (1995) Phenotype-specific expression of T-type calcium channels in neurons of the major pelvic ganglion of the adult male rat. *J Physiol* **489 (Pt 2)**:363-375.

JPET Fast Forward. Published on February 8, 2006 as DOI: 10.1124/jpet.105.098210
This article has not been copyedited and formatted. The final version may differ from this version.

Footnotes

This study was supported by a grant of the Korea Health 21 R&D project, Ministry of Health Welfare, Republic of Korea (03-PJ1-PG10-21300-0012). We thank Dr. Robert D. Wurst for proof-reading of this manuscript.

JPET Fast Forward. Published on February 8, 2006 as DOI: 10.1124/jpet.105.098210
This article has not been copyedited and formatted. The final version may differ from this version.

Legends for Figures

Fig 1. RT-PCR analysis of mRNAs encoding Ca^{2+} channel α1 subunits expressed in MPG neurons. Total RNA isolated from dissociated MPG neurons was reverse transcribed, and amplified by PCR with Ca^{2+} channel α1 subunit (α1A, α1B, α1C, α1D, α1E, and α1H)-specific primers (Table1). The resultant PCR products were separated and visualized on an agarose gel containing ethidium bromide. β-actin RNA as an internal control and whole brain RNA as a positive control were used. When the RT-PCR process was run without reverse transcriptase (RT-), no PCR products were observed indicating no contamination of genomic DNAs.

Fig. 2. HVA Ca^{2+} channel α1 subunits identified by Western blotting analysis in MPG neurons. Proteins extracted from MPG neurons and rat brain were probed with rabbit polyclonal antibodies directed against the II-III linkers of Ca^{2+} channel α1A, α1B, α1C, α1D, and α1E subunits. MPG neurons express all Ca^{2+} channel α1 subunits except α1A. The α1A antibody was able to reveal an appropriate band when applied to the brain proteins.

Fig. 3. Cell-specific functional markers expressed in MPG neurons. A, representative traces of inward Ca^{2+} currents in sympathetic and parasympathetic MPG neurons measured using whole cell patch clamp method. Ca^{2+} currents were evoked by a ramp

from -100 mV to +60 mV for 180 ms (upper traces) and test pulses to -30 mV (lower traces) from a holding potential of -100 mV. LVA T-type Ca^{2+} currents were exclusively detected as a hump or a transiently activating current in sympathetic MPG neurons. B, representative traces of inward Cl^- currents evoked by application of GABA (0.1mM) in MPG neurons held at -80 mV. The GABA response was significant in sympathetic MPG neurons, while negligible in parasympathetic MPG neurons. The GABA response was examined in the same cell where Ca^{2+} currents were recorded. The concentration of Cl^- was 20 mM in both internal and external solutions.

Fig. 4. Pharmacological dissection of HVA Ca^{2+} channel currents in MPG neurons. A, B, time courses of Ca^{2+} current block by serial application of nimodipine (10 μM), ω-contoxin GVIA (2 μM), ω-agatoxin IVA (1 μM), and $CdCl_2$ (0.1 mM) in sympathetic and parasympathetic MPG neurons, respectively. The peak Ca^{2+} current was evoked every 10 s by test pulses to +10 mV for 75 ms from a holding potential of -80 mV. *Inset*: current traces obtained at different time points (labeled a-e). C, summary of relative contribution of L-, N-, and R-type currents to total Ca^{2+} currents in sympathetic and parasympathetic MPG neurons. Data are presented as means±SEM. Number of cells tested is indicated in parentheses.

Fig. 5. Pharmacological characterization of R-type Ca^{2+} currents in MPG neurons. A,

JPET Fast Forward. Published on February 8, 2006 as DOI: 10.1124/jpet.105.098210
This article has not been copyedited and formatted. The final version may differ from this version.

effects of nickel and SNX-482 on R-type Ca^{2+} currents in a MPG neuron. In these experiments, L- and N-type Ca^{2+} currents were completely eliminated by application of nimodipine and ω-conotoxin GVIA prior to testing $NiCl_2$ (300 μM) and SNX-482 (500 nM). The peak Ca^{2+} current was evoked every 10 s by a test pulse to +10 mV for 75 ms from a holding potential of -80 mV. *Inset*: current traces obtained at different time points (labeled a-e). B, effects of nickel and SNX-482 on peak currents of the recombinant α1E Ca^{2+} channel. HEK 293 cells were transfected with 1, 0.5, 1, 0.7 μg of rat α_{1E}, rat β_{2a}, rat $\alpha_2\delta$, and GFP cDNAs, respectively, using calcium phosphate transfection method. Note that no endogenous currents were detected in HEK 293 control cells expressing only GFP. C, D, Concentration-response curves for block of the MPG R-type and the recombinant α1E Ca^{2+} currents by nickel and SNX-482. Note that the MPG R-type currents were minimally blocked by SNX-482 (500 nM). Absolute current block (%) was plotted as a function of drug concentration. Solid lines represent fits of experimental points by the Hill equation (see Material and Methods). For nickel block of MPG R-type and rbEII Ca^{2+} currents, IC_{50} values (Hill slope) were 22±0.1 μM (0.81±0.11) and 21±0.2 μM (0.75±0.13), respectively. For SNX-482 block of rbEII Ca^{2+} currents, the IC_{50} (Hill slope) was 76±0.4 nM (1.71±0.25). Data are presented as means±SEM.

JPET Fast Forward. Published on February 8, 2006 as DOI: 10.1124/jpet.105.098210
This article has not been copyedited and formatted. The final version may differ from this version.

Table 1. Ca^{2+} channel isoform-specific primers used for RT-PCR analysis

Primer	Accession #		Sequence	Predicted size
α1A	NM_012918	F	GATGAACAAGAAGAGGAAGAGG	332 bp
		R	CTTGTTGGTGTTGTTGTTACGG	
α1B	AF055477	F	TGGAGGGCTGGACTGACAT	282 bp
		R	GCGTTCTTGTCCTCCTCTGC	
α1C	M59786	F	AAGATGACTCCAACGCCACC	394 bp
		R	GATGATGACGAAGAGCACGAGG	
α1D	M57682	F	TGAGACACAGACGAAGCGAAGC	366 bp
		R	GTTGTCACTGTTGGCTATCTGG	
α1E	L15453	F	ATCTTACTGTGGACCTTCGTGC	506 bp
		R	CTCAGTGTAATGGATGCGCG	
α1H	AF290213	F	GCTCTCACCCGTCTACTTCG	256 bp
		R	AGATACTTTTCGCACGACCAGG	
β-actin	NM_031144	F	GGGAAATCGTGCGTGACATT	253 bp
		R	CGGATGTCAACGTCACACTT	

F : forward, R : reverse

Fig.1.

Fig.2.

Fig.3.

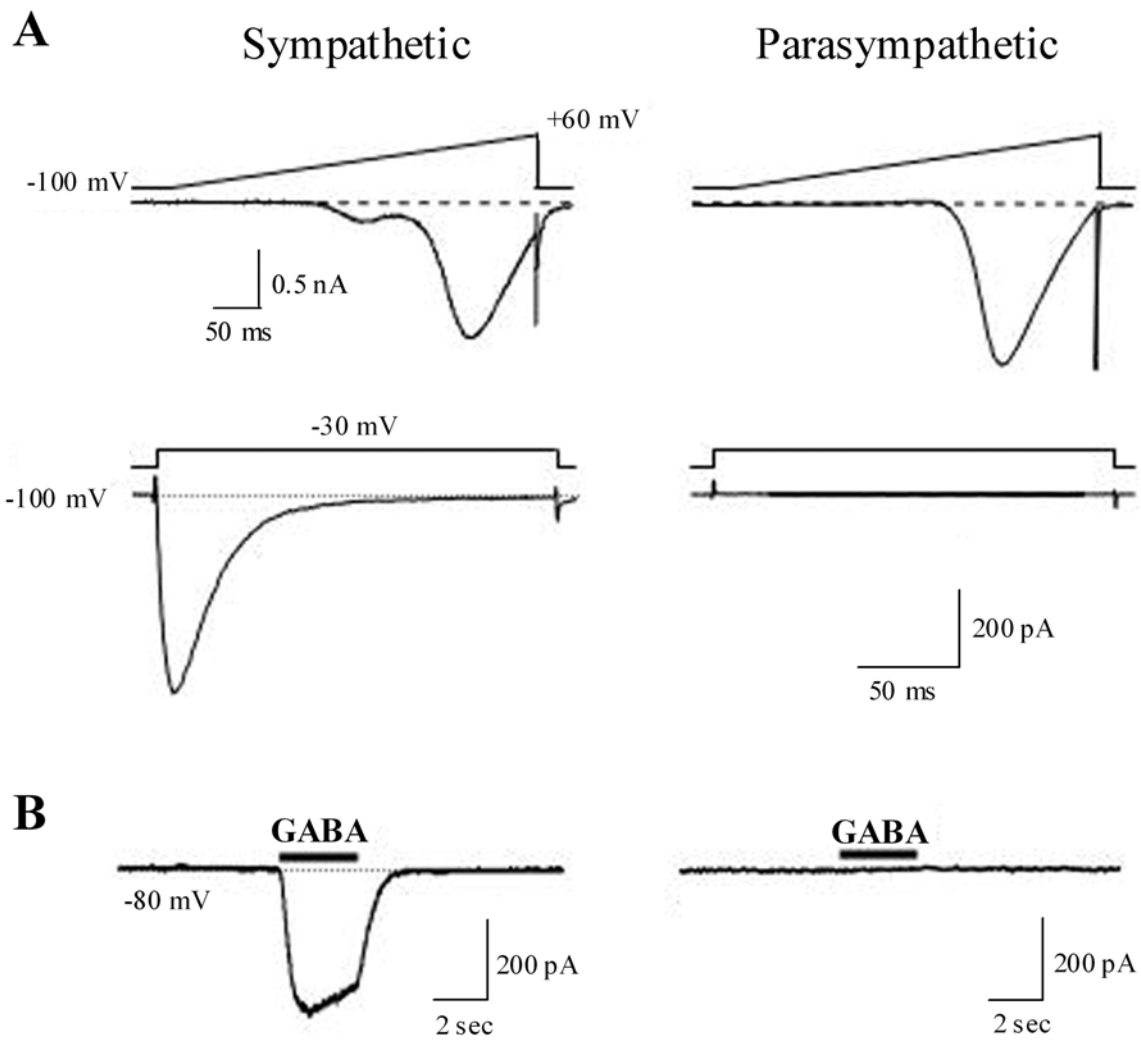

Fig.4.

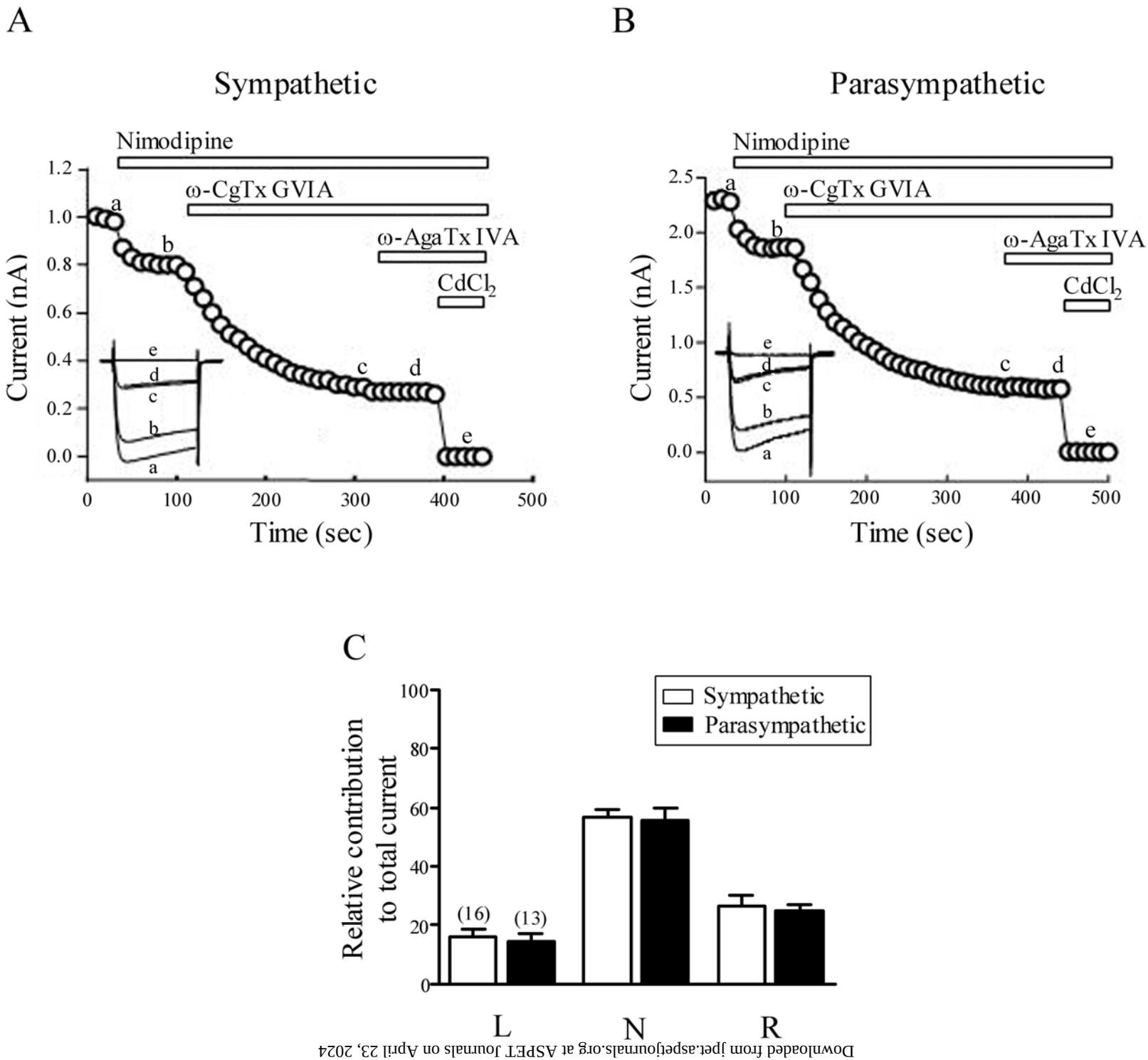

Fig.5.